iScience

CellPress
OPEN ACCESS

Article

Internal microbial zonation during the massive growth of marimo, a lake ball of *Aegagropila linnaei* in Lake Akan

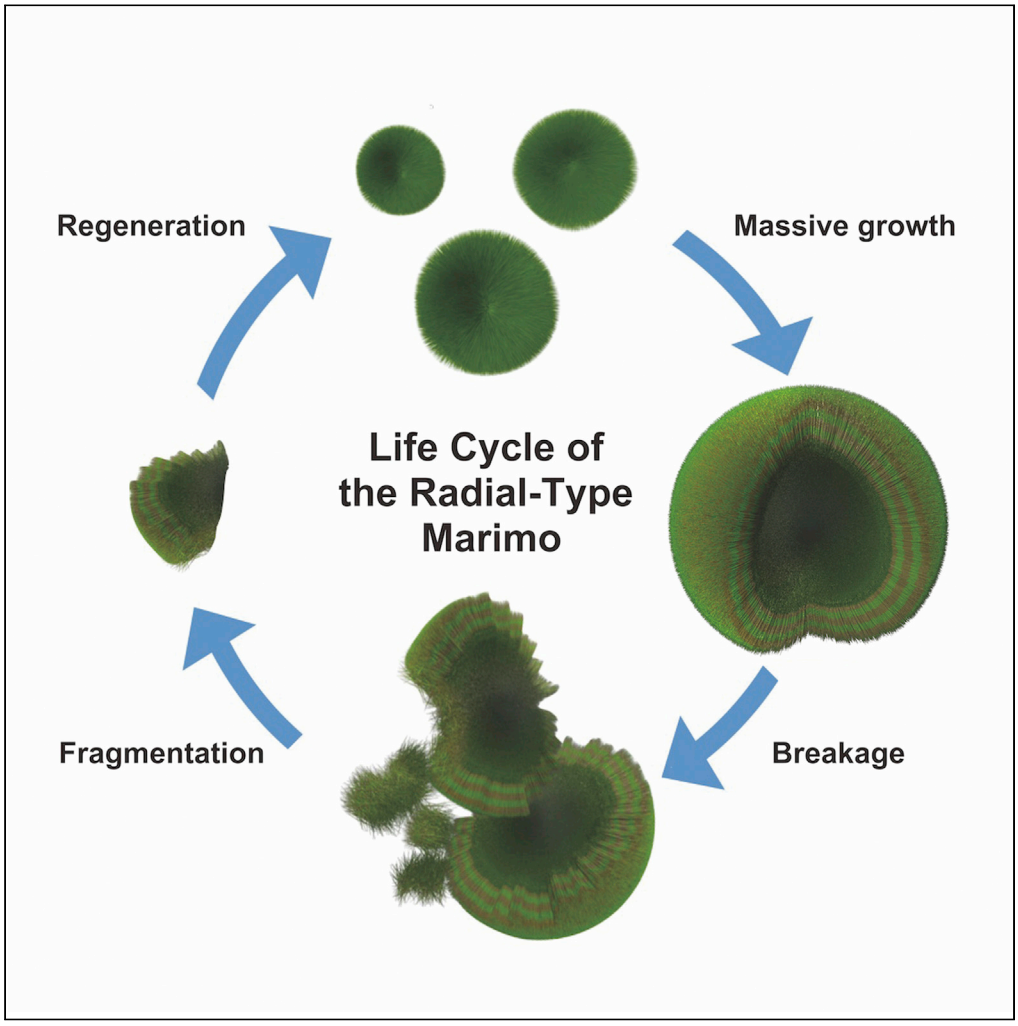

Ryosuke Nakai, Isamu Wakana, Hironori Niki

akantbe1@seagreen.ocn.ne.jp (I.W.)
hniki@nig.ac.jp (H.N.)

Highlights

The radial type of marimo (lake ball) can grow to over 20 cm in diameter

The sizable radial-type marimo develops the internal multi-layers and hollow structure

The layers provide different diverse microbiomes and structural strength

The internal multi-layers support the massive growth of the radial-type marimo

Nakai et al., iScience 24, 102720
July 23, 2021
https://doi.org/10.1016/j.isci.2021.102720

iScience

CellPress
OPEN ACCESS

Article

Internal microbial zonation during the massive growth of marimo, a lake ball of *Aegagropila linnaei* in Lake Akan

Ryosuke Nakai,[1,4] Isamu Wakana,[2,*] and Hironori Niki[1,3,5,*]

SUMMARY

Marimo (lake ball) is an uncommon ball-like aggregation of the green alga, *Aegagropila linnaei*. Although *A. linnaei* is distributed in fresh and brackish waters in the northern hemisphere, marimo colonies are found only in particular habitats. Here, we report the bacterial communities inside various sizes and aggregating structures of natural marimo collected from Lake Akan, Japan. We observed multi-layers composed of sediment particles only in the sizable radial-type marimo with >20 cm diameter and not in the tangled-type marimo. The deeper layers were enriched by *Nitrospira*, potential sulfur-oxidizing bacteria, and sulfate-reducing bacteria. Microorganisms of the multi-layers would form biofilms incorporating nearby sediment, which would function as microbial "seals" within large radial-type marimo. These findings provide clues to deciphering the growth of endangered marimo.

INTRODUCTION

Aegagropila linnaei, a filamentous green alga, widely inhabits ponds, lakes, and brackish waters at high latitudes in the northern hemisphere (Boedeker et al., 2010b). Morphologically, individuals of this species are filaments of 1–4 cm that are generally found attached to rocky substrates with rhizoids. This alga is known for an intriguing phenomenon in some lakes, including Lake Akan in Japan: it aggregates in spherical formations known as "lake balls" or "marimo" (Japanese for algal ball) (Soejima et al., 2009; Umekawa et al., 2021).

There are two structurally different types of marimo: the "tangled type" is an aggregate of disorderly entangled filaments, and the "radial type" is an aggregate of filaments radially arranged from the center to the surface (Horiguchi et al., 1998; Einarsson, 2014) (Figure 1). The size of the tangled type is usually several cm in diameter and not over 15 cm. On the other hand, the radial type develops into a sizable ball that occasionally reaches about 30 cm in diameter through the tip growth of the filaments (Horiguchi et al., 1998). Undoubtedly, the environmental conditions in habitats are significant determinants for the formation of the tangled- and radial-type marimo. Indeed, each type inhabits different areas of Lake Akan with different environmental conditions (Figure S1).

Recently, dense colonies of the radial-type marimo that grow over 10 cm in diameter have been found in two lakes, Lake Mývatn, Iceland, and Lake Akan (Einarsson et al., 2004), although this species inhabits many lakes. Regrettably, the marimo in Lake Mývatn has almost disappeared due to a deterioration of the environmental conditions (Einarsson, 2014). In Lake Akan, the dense colonies of the radial-type marimo are maintained within a restricted area at Churui Bay and Kinetanpe Bay.

It is known that external factors such as light, water quality, and water motion are involved in giving the marimo its spherical shape (Boedeker et al., 2010a; Sano et al., 2016). In addition to environmental conditions, we considered that various internal factors might be crucial for the more massive growth of the radial-type marimo. When the radial-type marimo inhabiting Lake Akan grows to about 10 cm in diameter, the filaments near its center begin to die, and a hollow is formed inside (Horiguchi et al., 1998). As a result, the densely packed filaments remain as an outer mass. These hollow structures are specific to the large aggregations of the radial-type marimo and are not formed in the smaller marimo of several cm in diameter. In a similar phenomenon, large aggregates of aquatic mosses are known to form "Koke-Bouzu" or large

[1]Microbial Physiology Laboratory, Department of Gene Function and Phenomics, National Institute of Genetics, 1111, Yata, Mishima, Shizuoka 411-8540 Japan

[2]Kushiro International Wetland Center, 7-5 Kuroganecho, Kushiro, Hokkaido 085-8505, Japan

[3]Department of Genetics, SOKENDAI (The Graduate University for Advanced Studies), 1111, Yata, Mishima, Shizuoka 411-8540 Japan

[4]Present address: Microbial Ecology and Technology Research Group, Bioproduction Research Institute, National Institute of Advanced Industrial Science and Technology (AIST), 2-17-2-1, Tsukisamu-higashi, Toyohira-ku, Sapporo, Hokkaido 062-8517 Japan

[5]Lead contact

*Correspondence: akantbe1@seagreen.ocn.ne.jp (I.W.), hniki@nig.ac.jp (H.N.)

https://doi.org/10.1016/j.isci.2021.102720

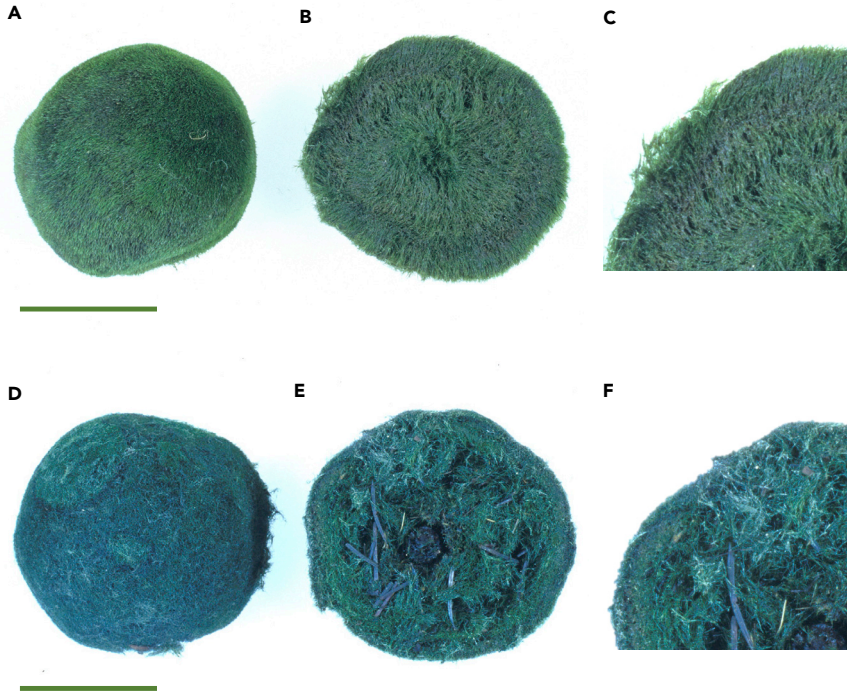

Figure 1. Two structurally different types of marimo from Lake Akan

Images of the radial-type marimo: (A) outward appearance, (B) a cross section showing the radial arrangement of filaments, (C) an enlarged cross section (×1.7). Images of the tangled-type marimo: (D) outward appearance, (E) a cross section showing the entanglement of pine leaves and an alder cone in the tangled filaments, (F) an enlarged cross section (×1.7). Scale bars, 5 cm.

pillar-like structures with an internal hollow at the bottom of ultraoligotrophic Antarctic lakes (Imura et al., 1999, 2000). The formation of the hollow structure in Koke-Bouzu is positively related to the internal microbiomes (Nakai et al., 2012). The interior of Koke-Bouzu is decomposed and rotten; redox potential gradients between this rotten interior and the exterior lead to a high diversity of microorganisms that are involved in material cycling in the *in situ* environment (Nakai et al., 2019). In addition to such moss-microbe associations, some bacteria co-existing with algae are known to exert beneficial effects on host growth through various symbiotic factors (e.g., nitrogen fixation and hormone production; Ramanan et al., 2016; Cirri and Pohnert, 2019). In some cases, the morphology and reproduction of a certain algal species are strongly dependent on the presence of bacteria (Tapia et al., 2016). Therefore, we presumed that the hollow structure and its associated microbiomes are related to the large size of the radial-type marimo.

RESULTS AND DISCUSSION

Dissection of natural marimo in Lake Akan

We dissected three differently sized natural samples of the radial-type marimo, each having a different internal structure and different redox conditions. Then, we examined the microbial communities in the outer and inner sections of these fresh marimo samples.

We collected the radial-type marimo at Churui Bay in Lake Akan and categorized them into three sizes: small (about 4 cm in diameter, $n = 3$), medium (11–12 cm in diameter, $n = 3$), and large (21 and 22 cm in diameter, $n = 2$). Each of the samples was cut to separate the outer and inner sections of the algal outer mass on a board immediately after the collection (Figure 2A). Using 16S ribosomal RNA (rRNA) gene-based sequencing of DNA samples extracted and pooled from each size fraction, we constructed bacterial catalogs for the sections of the marimo of different sizes, as well as for other samples, including a tangled-type marimo, a filament form, and the surrounding lake water and sediments, for comparison (Figure 2B and Tables S4, S5, S6, S7, S8, and S9). We excluded archaeal taxa from further analyses because they were poorly

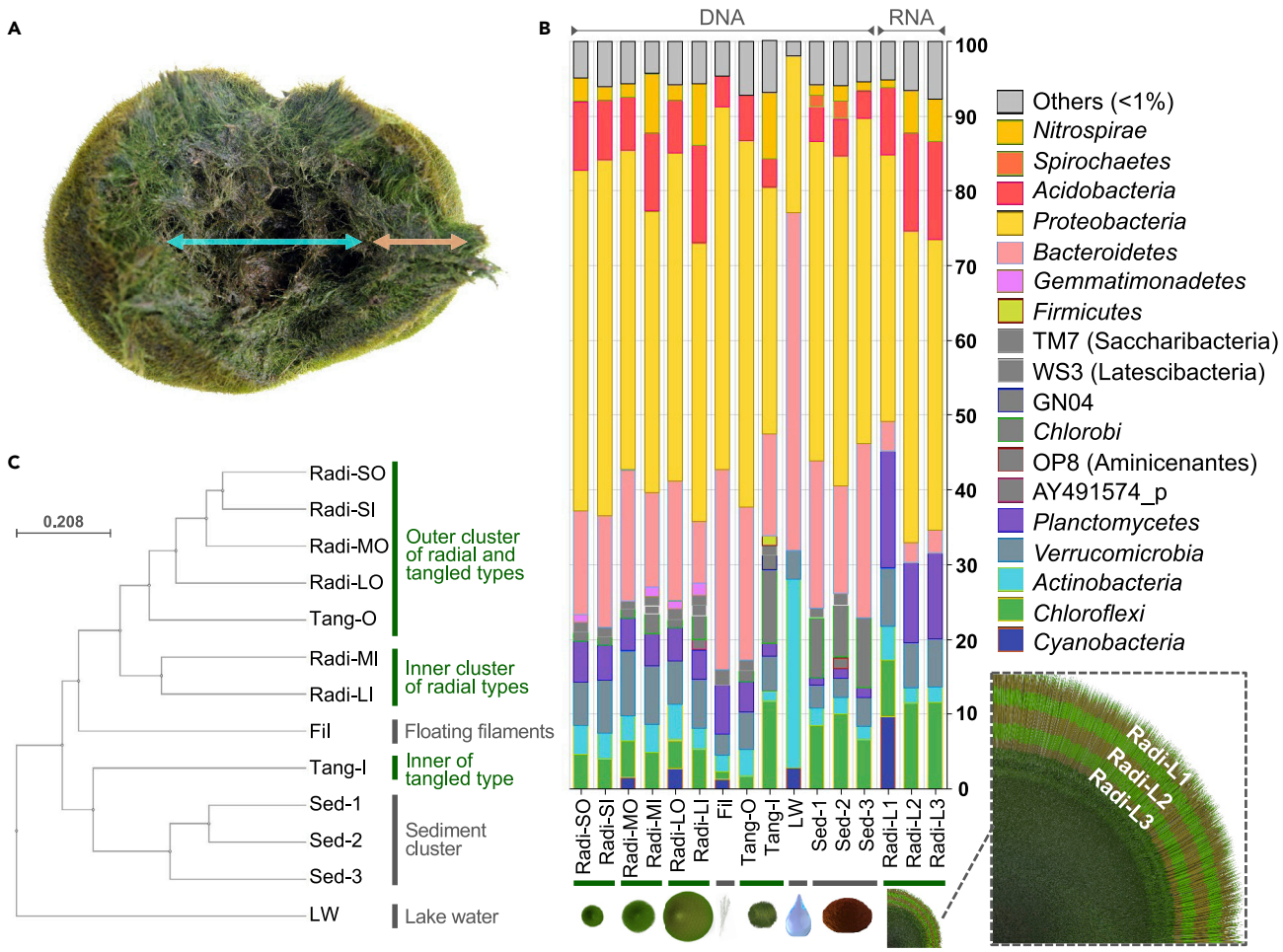

Figure 2. An integrated view of the phylogenetic diversity of the internal microbiomes of natural marimo

(A) Image of the interior structure of the radial-type marimo with a major axis of about 12 cm. The algal outer mass is indicated by an *orange arrow*, and the hollow structure is indicated by a *blue arrow*.

(B) Taxonomic composition of 13 bacterial phyla and 5 candidate phylum-level lineages (TM7, WS3, GN04, OP8, and AY491574_p) with >1% sequence abundance in at least one sample in DNA-based 16S rRNA gene amplicon data from radial-type marimo, floating filaments, tangled-type marimo, and other environmental samples, and RNA-based 16S rRNA transcript amplicon data from the multi-layers that developed only in the large radial-type marimo samples (see the layer structure presented in Figure 3). The outer sections of small-, medium-, and large-sized radial-type marimo are labeled Radi-SO, Radi-MO, and Radi-LO, respectively, and the inner sections are labeled Radi-SI, Radi-MI, and Radi-LI, respectively. Floating *A. linnaei* filaments and the outer and inner sections of the tangled-type marimo were labeled Fil, Tang-O, and Tang-I, respectively. Surface lake water and sediments surrounding the studied marimo colony were labeled LW, Sed-1, Sed-2, and Sed-3. The multi-layers (three layers), which were composed of sediment particles, were labeled Radi-L1, Radi-L2, and Radi-L3. Details for each sample are given in Table S1.

(C) A generalized UniFrac dendrogram showing similarities among the bacterial fractions of the microbiomes.

represented in our metabarcoding data. We found no apparent differences in the non-parametric Shannon diversity index (α-diversity) among the marimo microbiomes (Table S2). This result indicates that the species diversity of microbiomes is similar in the outer and inner sections. However, the β-diversity calculated by a generalized UniFrac dendrogram indicated apparent similarities and differences among bacterial communities of the marimo microbiomes (Figure 2C).

The phylogenetic diversity of the internal microbiomes of natural marimo

Microbiomes in the outer and inner sections of the small-sized marimo were similar. On the other hand, the microbiomes in the outer and inner sections of the medium- and large-sized marimo separated into respective clusters. We carried out a permutational multivariate analysis of variance analysis to assess statistical differences among the clusters in the UniFrac dendrogram (Figure 2C). The outer cluster of the radial

and tangled types trended toward a difference from the inner cluster of radial types ($p = 0.051$). The outer cluster was significantly different from the sediment cluster ($p < 0.01$). *Nitrospira* was frequently detected in the inner sections, while cyanobacteria were mainly found in the outer sections in the larger radial-type marimo (Figures 2B and Table S8). In particular, filamentous cyanobacterial members of *Nostocales* and *Oscillatoriales* were dominant (Table S6). Filamentous cyanobacteria are generally known to form benthic mats in aquatic environments, and their nitrogen-fixing capabilities are nutritionally significant in the biotic community (Paerl et al., 2000). In addition, we found bacteria related to the *Richelia* genus of the *Nostocales*, albeit at a low ratio (~0.1%) (Table S8). The bacteria of *Richelia* are known to promote host microalgal growth through symbiotic nitrogen fixation (Foster et al., 2011; Yao et al., 2019). Although Lake Akan is considered mesotrophic, it becomes nitrogen deficient in summer when aquatic plants and phytoplankton proliferate. Our measurements in Churui Bay, where we collected the marimo, showed that the concentrations of PO_4^{3-}, NH_4^+, NO_2^-, and NO_3^- in the surface water were below the detection limits (Table S3). Therefore, cyanobacterial N_2 fixation might help the marimo to grow under otherwise nitrogen-deficient conditions.

Meanwhile, nitrite-oxidizing *Nitrospira* members also can convert urea to NH_4^+ and CO_2 and are considered to contribute to nitrogen (N) cycling processes beyond nitrite oxidation (Koch et al., 2015). Thus, taxonomically different but functionally relevant (i.e., N cycle related) bacteria were consistently recovered from the outer and inner sections of the larger marimo. In contrast, such a distribution was not found in the smaller marimo. The UniFrac dendrogram also indicates that the microbiomes of the radial-type marimo were separately clustered with the other samples, including the surrounding lake water and sediments (Figure 2C). These results suggest that the radial-type marimo harbors unique and specific bacterial communities that assist in massive growth regardless of poor nutrient conditions.

Internal microbial zonation of the sizable radial-type marimo

We analyzed the interior structure of the radial-type marimo with a diameter of >20 cm. A cross section of the marimo showed that the algal outer mass developed to a thickness of about 2.5 cm, and the core part had a hollow. Additionally, we found multi-layers composed of accumulated brown-colored sediment particles inside the outer mass. Note that the sizable marimo populations distributed in shallow areas tend to be covered by lake sediments (Figure S2), while the attached sediments appear to be removed by the marimo's rotation. However, the sediment particles themselves are often sandwiched in layers within the algal outer mass. The large marimo we collected had a three-layered structure, and we named the layers Radi-L1 (0.3–0.4 cm deep from the surface), Radi-L2 (1 cm deep), and Radi-L3 (2 cm deep) (Figures 3A and S3). We then determined the composition of viable and active microbiomes in these multi-layers by means of RNA-based metabarcoding of the 16S rRNA transcripts. While DNA-based analysis cannot differentiate live and dead bacterial cells, RNA-based analysis can identify live bacteria because RNA is degraded after cell death (Bleve et al., 2003; Li et al., 2017). The results of the RNA-based metabarcoding analysis showed that (1) *Proteobacteria* was dominant in Radi-L1, Radi-L2, and Radi-L3, as shown in the results of the DNA-based analysis, (2) *Chloroflexi* and *Planctomycetes* were subdominant in all layers, and (3) *Cyanobacteria* was prominent only in Radi-L1 (Figure 2B).

Moreover, distinctive distributions of certain taxa were found in each layer. Some of the dominant bacterial genera and genus-level lineages differed between the surface layer, Radi-L1, and the deeper layers, Radi-L2 and Radi-L3 (Figure 3B). In Radi-L1, a novel cyanobacterial lineage within the *Symploca*-related family was frequently detected. The novel δ-proteobacterial lineage AJ617907_g of *Polyangiaceae* and α-proteobacterial *Hyphomicrobium* were also detected. In contrast, these members were minor components (<0.2%) in the Radi-L2 and Radi-L3 layers. *Symploca* spp. are aerobic, filamentous N_2-fixing cyanobacteria that occur in microbial mats (Stal, 2012). The δ-proteobacterial AJ617907 sequence was initially discovered from the oxic-anoxic interphase of soil (DDBJ/ENA/GenBank: AJ617907). Members of *Hyphomicrobium* are considered to be significant players in denitrification (Martineau et al., 2015), which is a microbial process of converting NO_2^- and NO_3^- to N_2 under oxygen-limiting conditions. The detection of these viable and active members suggests that an O_2 concentration gradient might be formed in the surface layer Radi-L1.

Unique microbiome in the deeper layers of the sizable radial-type marimo

On the other hand, a novel γ-proteobacterial group within the *Sedimenticola*-related family, the δ-proteobacterial AXXL_g of *Desulfobacteraceae*, *Nitrospira*, and other multiple uncultured lineages dominated in both Radi-L2 and Radi-L3 (Figure 3B). The novel γ-proteobacterial group and *Nitrospira* were highly

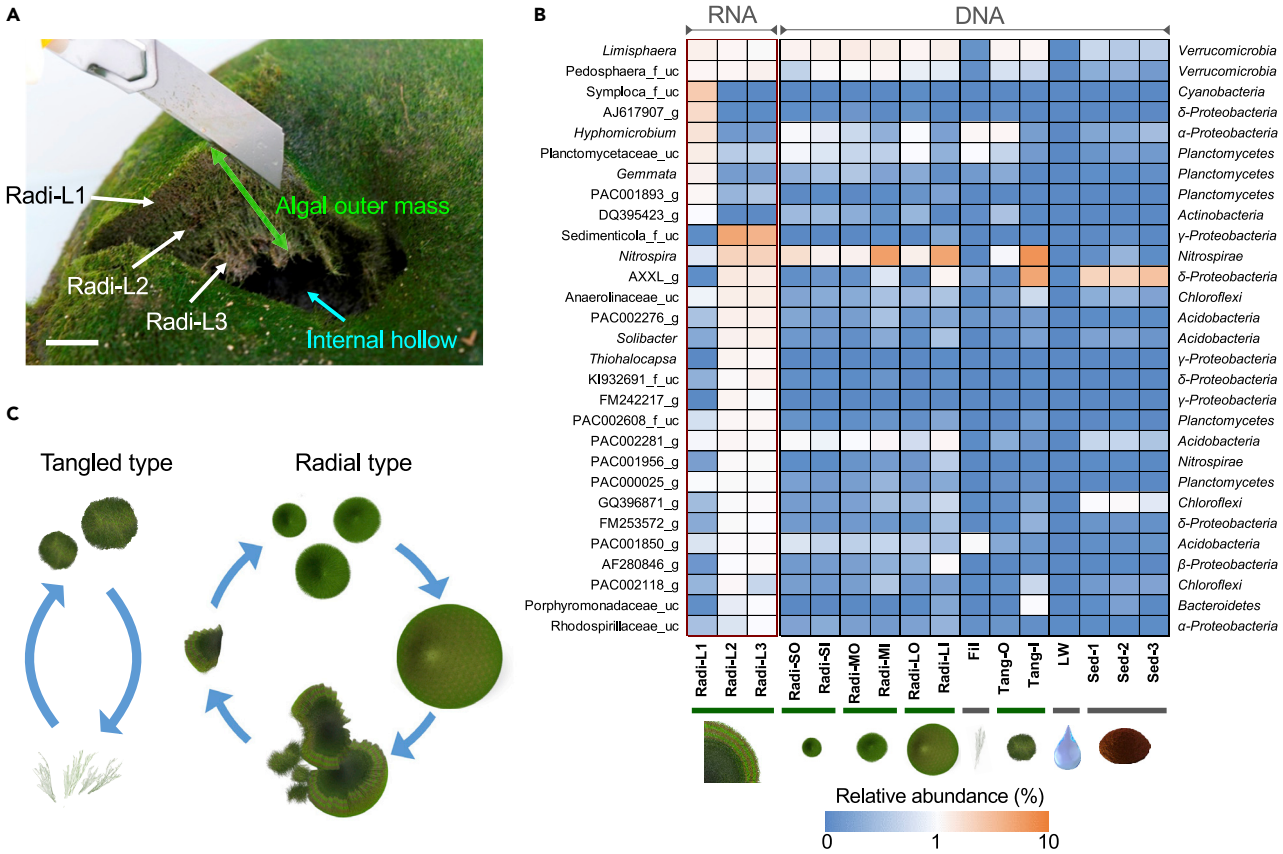

Figure 3. Multi-layers, internal microbial zonation, and proposed development process of the sizable radial-type marimo

(A) Image of three brown-colored layers inside the algal outer mass and the internal hollow of the large-sized, radial-type marimo with a diameter of >20 cm. The three layers were labeled Radi-L1 (0.3–0.4 cm deep from the surface), Radi-L2 (1 cm deep), and Radi-L3 (2 cm deep). Scale bar, 1 cm.

(B) Heatmap showing 6 genera (*Limisphaera*, *Hyphomicrobium*, *Gemmata*, *Nitrospira*, *Solibacter*, and *Thiohalocapsa*) and 23 other unclassified or candidate genus-level lineages with >1% sequence abundance in at least one sample in RNA-based 16S rRNA transcript amplicon data from the multi-layers. The frequency of occurrence of each lineage in other samples obtained from DNA-based 16S rRNA gene amplicon data is also shown. Sample name codes are presented in Figure 2 and Table S1. EzTaxon category names and taxonomic affiliations at the phylum or class level (for *Proteobacteria*) are shown on the left and the right side, respectively. Note that reclassification of the δ-proteobacterial members has recently been proposed (Waite et al., 2020). Following the EzBioCloud database, the uncultured phylotype is tentatively given the hierarchical name assigned to the DDBJ/ENA/GenBank accession number with the following suffixes: "_s" (for species), "_g" (genus), "_f" (family), "_o" (order), "_c" (class), and "_p" (phylum). The unclassified sequences below the cut-off values are labeled "_uc" (for unclassified).

(C) Models of development and regeneration of the tangled-type and radial-type marimo. For the tangled-type marimo, *A. linnaei* filaments cycle between a free-floating state and an entangled state (*left*). The radial-type marimo is regenerated from a fragment derived from a broken larger radial-type individual so that the radial arrangements of filaments and the inside microbiomes are inherited (*right*).

enriched in Radi-L2 and Radi-L3 (6.1–7.1% and 3.9–4.0%, respectively) and were minor in Radi-L1 (0.03% and 0.8%, respectively). Known *Sedimenticola* strains are chemoautotrophic bacteria and can utilize sulfur compounds (e.g., elemental sulfur and hydrogen sulfide) (Flood et al., 2015). They fall within the unclassified γ-*Proteobacteria* monophyletic clade with multiple microaerobic sulfur-oxidizing endosymbionts of marine invertebrates (e.g., bivalve molluscs) endemic to sulfidic environments (Dubilier et al., 2008). The majority of the sequences of the novel γ-proteobacterial group had 93–94% similarity with the marine sediment sequence (DDBJ/ENA/GenBank: JF344428). Their closest type strain was *Sulfurivermis fontis* JG42^{T}, which is a sulfur-oxidizing autotroph that was isolated from a hot spring microbial mat (Kojima et al., 2017). The novel member inhabiting the marimo deeper layers might have a sulfur-related chemoautotrophic metabolism.

Filaments in the inner sections maintain their green color, indicating that chloroplasts remain despite the darkness within the marimo (Figure 3A). When the inner filaments are isolated and irradiated with light,

the photosynthesis activity recovers within a few days (Yokohama et al., 1994; Horiguchi et al., 1998). Thus, the photosynthetic activity of the radial-type marimo decreases from the surface to the interior, but the inner filaments are somehow viable. In this context, potential chemoautotrophic bacteria identified in the inner sections may carry out chemosynthetic CO_2 fixation. Then, the primary production by the CO_2 fixation may contribute to the survival of inner filaments in the marimo interior. Remarkably, Lake Akan is rich in sulfur and hydrogen sulfide, which sulfur-oxidizing bacteria can use, due to the inflow of water from a river associated with a nearby volcano, Mt. Me-Akan (Suzuki et al., 1957; Japan Wildlife Research Center, 2015).

Moreover, an uncultured lineage AXXL_g dominantly detected in the deeper layers of Radi-L2 and Radi-L3 belongs to *Desulfobacteraceae* within *δ-Proteobacteria*. Most of the *Desulfobacteraceae* species are sulfate-reducing anaerobes (Kuever, 2014). The AXXL_g-related sequences were found in the sediments surrounding the marimo colonies (Figure 3B). Other lineages, such as GQ396871_g of *Chloroflexi* in Radi-L2 and Radi-L3 were also enriched in the nearby sediments. The spatial distributions suggested that the two deeper layers possess anaerobic microenvironments which sediment bacteria can inhabit.

The microbial zonation as a mechanical structure

It is worth noting that the filamentous cyanobacteria on the marimo surface might be involved in not only CO_2 and N_2 fixation but also the incorporation of minerals and organic matter. Furthermore, the filamentous microorganisms produce extracellular polymeric substances and release them into their surroundings (Stal, 2012). The surfaces of *A. linnaei* filaments isolated from the radial-type marimo are known to be highly sticky. Cyanobacteria-mediated formation of microbial granules and biofilms is often observed in nutrient-limited glaciers and polar freshwater lakes (Uetake et al., 2016; Jungblut and Vincent, 2017). In addition, many of the *Acidobacteria* that were frequently detected in both Radi-L2 and Radi-L3 (Figure 3B) have the potential to form biofilms and facilitate particle aggregates (Kielak et al., 2016). Thus, it is possible that "microbial sealing" by bacterial aggregates/biofilms enhances the beneficial effects on the strength of the multi-layers inside marimo. In fact, sizable radial-type marimo are airtight and rigid structures (Figure S4 and Video S1). It is difficult for water to enter the internal cavity. Once the inside water is removed, the marimo floats on water for days (Figure S4C).

The development process and the life cycles of the radial-type marimo

Physical factors in the growing environment are involved in the developmental mechanism of the ball-like marimo. Wind waves are a driving force which rotates marimo and maintains their rounded spherical form (Sano et al., 2016). The rotation of marimo enables photosynthesis over the entire marimo surface and removes sediment from the surface. However, the tangled-type marimo cannot grow into a larger aggregate of over 20 cm in diameter like the radial-type marimo. Only the actively growing marimo over 20 cm in diameter develops the internal multi-layers. The layers are available for habitats of distinctive bacteria. As a result, the bacterial zonation would supply carbon sources and nutrients to the host *A. linnaei* and promote the massive growth of the radial-type marimo. In addition, the microbial sealing of the layer structure could confer mechanical strength to the radial-type marimo. A possible scenario of the regeneration of a radial-type marimo is as follows (Figure 3C). First, an extremely large marimo is broken down and fragmented by external forces such as turbulent water movements (Figure S2A). Fragments of the large aggregate then reform as a small marimo which inherits the radial arrangements of filaments and the interior microbiomes.

Environmental eutrophication affects not only the algal growth but also the microbial community inside the marimo. Understanding both the external factors and the functioning of the internal microbiomes will aid in the management of these globally endangered organisms.

Limitations of the study

Due to the challenge created by the limited number of marimo samples available for analysis, inter-individual differences and seasonal variations in the marimo microbiomes were not elucidated. Species diversity and host associations of eukaryotic microorganisms, which were not targeted in this study, also merit investigation in order to clarify the contribution of the microbiome to algal growth.

STAR★METHODS

Detailed methods are provided in the online version of this paper and include the following:

- KEY RESOURCES TABLE
- RESOURCE AVAILABILITY
  - Lead contact
  - Materials availability
  - Data and code availability
- EXPERIMENTAL MODEL AND SUBJECT DETAILS
  - Sample collection
- METHOD DETAILS
  - Evaluation of lake water quality
  - DNA extraction, PCR amplification, and high-throughput sequencing
  - RNA extraction and cDNA synthesis
  - Data analysis
- QUANTIFICATION AND STATISTICAL ANALYSIS

SUPPLEMENTAL INFORMATION

Supplemental information can be found online at https://doi.org/10.1016/j.isci.2021.102720.

ACKNOWLEDGMENTS

We are deeply grateful to Drs. S. Imura and M. Tsujimoto for their invaluable help with the field sampling and diving. This work was partly supported by the Systematic Analysis for Global environmental change and life on Earth (SAGE) project promoted by the Trans-disciplinary Research Integration Center, under the umbrella of the Research Organization of Information and Systems, Japan. This work was partly supported by a Grant-in-Aid for Scientific Research from the Japan Society for the Promotion of Science (no. JP15H05620 to R.N.).

AUTHOR CONTRIBUTIONS

R.N. and H.N. coordinated the study. All authors conducted field studies. R.N. conducted microbiome experiments and data analysis. I.W. has observed the life cycles of marimo for many years and took all our underwater photos of the marimo in Lake Akan by scuba diving. All authors discussed the data, wrote the manuscript, and approved the final version.

DECLARATION OF INTERESTS

The authors declare no competing interests.

Received: March 20, 2021
Revised: May 24, 2021
Accepted: June 9, 2021
Published: July 23, 2021

REFERENCES

Anderson, M.J. (2017). Permutational Multivariate Analysis of Variance (PERMANOVA) (Wiley Statsref: Statistics Reference Online), pp. 1–15. https://doi.org/10.1002/9781118445112.stat07841.

Aronesty, E. (2013). Comparisons of sequencing utility programs. Open Bioinform. J. *7*, 1–8. https://doi.org/10.2174/1875036201307010001.

Bleve, G., Rizzotti, L., Dellaglio, F., and Torriani, S. (2003). Development of reverse transcription (RT)-PCR and real-time RT-PCR assays for rapid detection and quantification of viable yeasts and molds contaminating yogurts and pasteurized food products. Appl. Environ. Microbiol. *69*, 4116–4122. https://doi.org/10.1128/aem.69.7.4116-4122.2003.

Boedeker, C., Eggert, A., Immers, A., and Smets, E. (2010a). Global decline of and threats to *Aegagropila linnaei*, with special reference to the lake ball habit. BioScience *60*, 187–198. https://doi.org/10.1525/bio.2010.60.3.5.

Boedeker, C., Eggert, A., Immers, A., and Wakana, I. (2010b). Biogeography of *Aegagropila linnaei* (Cladophorophyceae, Chlorophyta): a widespread freshwater alga with low effective dispersal potential shows a glacial imprint in its distribution. J. Biogeogr. *37*, 1491–1503. https://doi.org/10.1111/j.1365-2699.2010.02309.x.

Bolger, A.M., Lohse, M., and Usadel, B. (2014). Trimmomatic: a flexible trimmer for Illumina sequence data. Bioinformatics *30*, 2114–2120. https://doi.org/10.1093/bioinformatics/btu170.

Chao, A. (1984). Nonparametric estimation of the number of classes in a population. Scand. J. Statist. *11*, 265–270.

Chao, A., and Shen, T.J. (2003). Nonparametric estimation of Shannon's index of diversity when there are unseen species in sample. Environ. Ecol. Stat. *10*, 429–443. https://doi.org/10.1023/A:1026096204727.

Chen, J., Bittinger, K., Charlson, E.S., Hoffmann, C., Lewis, J., Wu, G.D., Collman, R.G., Bushman, F.D., and Li, H. (2012). Associating microbiome composition with environmental covariates using generalized UniFrac distances. Bioinformatics *28*, 2106–2113. https://doi.org/10.1093/bioinformatics/bts342.

Cirri, E., and Pohnert, G. (2019). Algae–bacteria interactions that balance the planktonic microbiome. New Phytol. *223*, 100–106. https://doi.org/10.1111/nph.15765.

Dubilier, N., Bergin, C., and Lott, C. (2008). Symbiotic diversity in marine animals: the art of harnessing chemosynthesis. Nat. Rev. Microbiol. *6*, 725–740. https://doi.org/10.1038/nrmicro1992.

Edgar, R.C. (2010). Search and clustering orders of magnitude faster than BLAST. Bioinformatics *26*, 2460–2461. https://doi.org/10.1093/bioinformatics/btq461.

Edgar, R.C., Haas, B.J., Clemente, J.C., Quince, C., and Knight, R. (2011). UCHIME improves sensitivity and speed of chimera detection. Bioinformatics *27*, 2194–2200. https://doi.org/10.1093/bioinformatics/btr381.

Einarsson, Á., Stefánsdóttir, G., Jóhannesson, H., Ólafsson, J.S., Gíslason, G.M., Wakana, I., Gudbergsson, G., and Gardarsson, A. (2004). The ecology of Lake myvatn and the river laxá: variation in space and time. Aquat. Ecol. *38*, 317–348. https://doi.org/10.1023/B:AECO.0000032090.72702.a9.

Einarsson, Á. (2014). The Lake Balls of Mývatn in Memoriam. Mývatn Research Station. https://www.ramy.is/wordpress/wp-content/uploads/2014/05/Lake_Ball_in_memoriam_final_draft_reduced_size2.pdf.

Flood, B.E., Jones, D.S., and Bailey, J.V. (2015). *Sedimenticola thiotaurini* sp. nov., a sulfur-oxidizing bacterium isolated from salt marsh sediments, and emended descriptions of the genus *Sedimenticola* and *Sedimenticola selenatireducens*. Int. J. Syst. Evol. Microbiol. *65*, 2522–2530. https://doi.org/10.1099/ijs.0.000295.

Foster, R.A., Kuypers, M.M., Vagner, T., Paerl, R.W., Musat, N., and Zehr, J.P. (2011). Nitrogen fixation and transfer in open ocean diatom–cyanobacterial symbioses. ISME J. *5*, 1484–1493. https://doi.org/10.1038/ismej.2011.26.

Good, I.J. (1953). The population frequencies of species and the estimation of population parameters. Biometrika *40*, 237–264. https://doi.org/10.1093/biomet/40.3-4.237.

Horiguchi, T., Yoshida, T., Nagao, M., Wakana, I., and Yokohama, Y. (1998). Ultrastructure of chloroplasts in 'Marimo' (*Cladophora aegagropila*, Chlorophyta), and changes after exposure to light. Psychol. Res. *46*, 253–261. https://doi.org/10.1046/j.1440-1835.1998.00143.x.

Imura, S., Bando, T., Saito, S., Seto, K., and Kanda, H. (1999). Benthic moss pillars in Antarctic lakes. Polar Biol. *22*, 137–140. https://doi.org/10.1007/s003000050401.

Imura, S., Takahashi, H., and Nakamura, T. (2000). Benthic moss pillars (Koke Bouzu) in Antarctic lakes–analysis of colonization and growth by 14C dating. Sum. Res. AMS, Nagoya Univ. *11*, 176–183. https://doi.org/10.18999/sumrua.11.176.

Japan Wildlife Research Center (2015). Akan, Kussharo, Mashu. Reports for World natural heritage candidate sites 52–68. https://www.env.go.jp/nature/report/h26-05/full.pdf.

Jungblut, A.D., and Vincent, W.F. (2017). Cyanobacteria in polar and alpine ecosystems. In Psychrophiles: From Biodiversity to Biotechnology, R. Margesin, ed. (Springer), pp. 181–206. https://doi.org/10.1007/978-3-319-57057-0_9.

Kielak, A.M., Barreto, C.C., Kowalchuk, G.A., van Veen, J.A., and Kuramae, E.E. (2016). The ecology of *Acidobacteria*: moving beyond genes and genomes. Front. Microbiol. *7*, 744. https://doi.org/10.3389/fmicb.2016.00744.

Kim, O.S., Cho, Y.J., Lee, K., Yoon, S.H., Kim, M., Na, H., Park, S.C., Jeon, Y.S., Lee, J.H., Yi, H., et al. (2012). Introducing EzTaxon-e: a prokaryotic 16S rRNA gene sequence database with phylotypes that represent uncultured species. Int. J. Syst. Evol. Microbiol. *62*, 716–721. https://doi.org/10.1099/ijs.0.038075-0.

Koch, H., Lücker, S., Albertsen, M., Kitzinger, K., Herbold, C., Spieck, E., and Daims, H. (2015). Expanded metabolic versatility of ubiquitous nitrite-oxidizing bacteria from the genus *Nitrospira*. Proc. Natl. Acad. Sci. U S A *112*, 11371–11376. https://doi.org/10.1073/pnas.1506533112.

Kojima, H., Watanabe, M., and Fukui, M. (2017). *Sulfurivermis fontis* gen. nov., sp. nov., a sulfur-oxidizing autotroph, and proposal of *Thioprofundaceae* fam. nov. Int. J. Syst. Evol. Microbiol. *67*, 3458–3461. https://doi.org/10.1099/ijsem.0.002137.

Kuever, J. (2014). The family *Desulfobacteraceae*. In The Prokaryotes., E. Rosenberg, E.F. DeLong, F. Thompson, S. Lory, E. Stackebrand, and D. Quinones, eds. (Springer), pp. 45–73. https://doi.org/10.1007/978-3-642-39044-9_266.

Li, R., Tun, H.M., Jahan, M., Zhang, Z., Kumar, A., Fernando, D., Farenhorst, A., and Khafipour, E. (2017). Comparison of DNA-, PMA-, and RNA-based 16S rRNA Illumina sequencing for detection of live bacteria in water. Sci. Rep. *7*, 1–11. https://doi.org/10.1038/s41598-017-02516-3.

Martin, M. (2011). Cutadapt removes adapter sequences from high-throughput sequencing reads. Embnet J. *17*, 10–12. https://doi.org/10.14806/ej.17.1.200.

Martineau, C., Mauffrey, F., and Villemur, R. (2015). Comparative analysis of denitrifying activities of *Hyphomicrobium nitrativorans*, *Hyphomicrobium denitrificans*, and *Hyphomicrobium zavarzinii*. Appl. Environ. Microbiol. *81*, 5003–5014. https://doi.org/10.1128/AEM.00848-15.

Mori, H., Maruyama, F., Kato, H., Toyoda, A., Dozono, A., Ohtsubo, Y., Nagata, Y., Fujiyama, A., Tsuda, M., and Kurokawa, K. (2014). Design and experimental application of a novel non-degenerate universal primer set that amplifies prokaryotic 16S rRNA genes with a low possibility to amplify eukaryotic rRNA genes. DNA Res. *21*, 217–227. https://doi.org/10.1093/dnares/dst052.

Nakai, R., Abe, T., Baba, T., Imura, S., Kagoshima, H., Kanda, H., Kanekiyo, A., Kohara, Y., Koi, A., Nakamura, K., et al. (2012). Microflorae of aquatic moss pillars in a freshwater lake, East Antarctica, based on fatty acid and 16S rRNA gene analyses. Polar Biol. *35*, 425–433. https://doi.org/10.1007/s00300-011-1090-2.

Nakai, R., Imura, S., and Naganuma, T. (2019). Patterns of microorganisms inhabiting antarctic freshwater lakes with special reference to aquatic moss pillars. In The Ecological Role of Micro-organisms in the Antarctic Environment, S. Castro-Sowinski, ed. (Springer), pp. 25–43. https://doi.org/10.1007/978-3-030-02786-5_2.

Paerl, H.W., Pinckney, J.L., and Steppe, T.F. (2000). Cyanobacterial-bacterial mat consortia: examining the functional unit of microbial survival and growth in extreme environments. Environ. Microbiol. *2*, 11–26. https://doi.org/10.1046/j.1462-2920.2000.00071.x.

Ramanan, R., Kim, B.H., Cho, D.H., Oh, H.M., and Kim, H.S. (2016). Algae–bacteria interactions: evolution, ecology and emerging applications. Biotechnol. Adv. *34*, 14–29. https://doi.org/10.1016/j.biotechadv.2015.12.003.

Sano, F., Nakayama, K., Yamada, T., Sato, Y., Maruyama, Y., Komai, K., Oyama, Y., and Wakana, I. (2016). Project of wind waves which induce rotary motion of marimo in Lake Akan. Ann. J. Civil Eng. Ocean *72*, I_988–I_993. https://doi.org/10.2208/jscejoe.72.I_988.

Soejima, A., Yamazaki, N., Nishino, T., and Wakana, I. (2009). Genetic variation and structure of the endangered freshwater benthic alga Marimo, *Aegagropila linnaei* (Ulvophyceae) in Japanese lakes. Aquat. Ecol. *43*, 359–370. https://doi.org/10.1007/s10452-008-9204-9.

Stal, L.J. (2012). Cyanobacterial mats and stromatolites. In Ecology of Cyanobacteria II, B. Whitton, ed. (Springer), pp. 65–125. https://doi.org/10.1007/0-306-46855-7_4.

Suzuki, J., Ishikawa, T., Ômachi, H., and Suzuki, Y. (1957). On the sulphur deposits of the Akan sulphur mine. J. Fac. Sci. Hokkaido Univ. Ser. *4 9*, 501–518.

Tapia, J.E., González, B., Goulitquer, S., Potin, P., and Correa, J.A. (2016). Microbiota influences morphology and reproduction of the Brown alga *ectocarpus* sp. Front. Microbiol *7*, 197. https://doi.org/10.3389/fmicb.2016.00197.

Uetake, J., Tanaka, S., Segawa, T., Takeuchi, N., Nagatsuka, N., Motoyama, H., and Aoki, T. (2016). Microbial community variation in cryoconite granules on Qaanaaq Glacier, NW Greenland. FEMS Microbiol. Ecol. *92*, fiw127. https://doi.org/10.1093/femsec/fiw127.

Umekawa, T., Wakana, I., and Ohara, M. (2021). Reproductive behavior and role in maintaining an aggregative form of the freshwater green alga Marimo, *Aegagropila linnaei*, in Lake Akan, Hokkaido, Japan. Aquat. Bot. *168*, 103309. https://doi.org/10.1016/j.aquabot.2020.103309.

Unno, T. (2015). Bioinformatic suggestions on MiSeq-based microbial community analysis. J. Microbiol. Biotechnol. *25*, 765–770. https://doi.org/10.4014/jmb.1409.09057.

Waite, D.W., Chuvochina, M., Pelikan, C., Parks, D.H., Yilmaz, P., Wagner, M., Loy, A., Naganuma, T., Nakai, R., Whitman, W.B., et al. (2020). Proposal to reclassify the proteobacterial classes *Deltaproteobacteria* and *Oligoflexia*, and the phylum *Thermodesulfobacteria* into four phyla reflecting major functional capabilities. Int. J. Syst. Evol. Microbiol. *70*, 5972–6016. https://doi.org/10.1099/ijsem.0.004213.

Yao, S., Lyu, S., An, Y., Lu, J., Gjermansen, C., and Schramm, A. (2019). Microalgae–bacteria symbiosis in microalgal growth and biofuel production: a review. J. Appl. Microbiol. *126*, 359–368. https://doi.org/10.1111/jam.14095.

Yarza, P., Yilmaz, P., Pruesse, E., Glöckner, F.O., Ludwig, W., Schleifer, K.H., Whitman, W.B., Euzeby, J., Amann, R., and Rossello-Mora, R. (2014). Uniting the classification of cultured and uncultured bacteria and archaea using 16S rRNA gene sequences. Nat. Rev. Microbiol. *12*, 635–645. https://doi.org/10.1038/nrmicro3330.

Yokohama, Y., Nagao, M., and Wakana, I. (1994). Photosynthetic pigments in spherical aggregation of "Marimo". Marimo Res. *3*, 12–15.

Yoon, S.H., Ha, S.M., Kwon, S., Lim, J., Kim, Y., Seo, H., and Chun, J. (2017). Introducing EzBioCloud: a taxonomically united database of 16S rRNA gene sequences and whole-genome assemblies. Int. J. Syst. Evol. Microbiol. *67*, 1613–1617. https://doi.org/10.1099/ijsem.0.001755.

STAR★METHODS

KEY RESOURCES TABLE

REAGENT or RESOURCE	SOURCE	IDENTIFIER
Biological samples		
Marimo samples, see Table S1	Lake Akan, Japan	43° 27′ N 144° 06′ E
Sediment samples, see Table S1	Lake Akan, Japan	43° 27′ N 144° 06′ E
Lake water sample, see Table S1	Lake Akan, Japan	43° 27′ N 144° 06′ E
Critical commercial assays		
RNA*later*	Thermo Fisher Scientific	Cat# AM7020
Lysing Matrix E Tube	MP Biomedicals	Cat# 116914050
ISOIL for Beads Beating Kit	Nippon Gene	Cat# 319-06201
MagExtractor Genome Kit	Toyobo	Cat# NPK-101
KAPA HiFi HotStart ReadyMix (2X)	Kapa Biosystems	Cat# KK2601
Nextera XT Index Kit	illumina	Cat# FC-131-1002
16S Metagenomic Sequencing Library Preparation	illumina	https://jp.support.illumina.com/downloads/16s_metagenomic_sequencing_library_preparation.html
PowerWater Sterivex DNA Isolation Kit	MP Biomedicals	Cat# 14600-50-NF
FastRNA Pro Soil-Direct Kit	MP Biomedicals	Cat# 6070-050
TURBO DNA-*free* Kit	Thermo Fisher Scientific	Cat# AM1907
SuperScript VILO cDNA Synthesis Kit and Master Mix	Thermo Fisher Scientific	Cat# 11752050
Deposited data		
Raw sequence data	This study	DDBJ Sequence Read Archive (DRA): DRA010176
Project data	This study	BioProject: PRJDB8727
Sample data, see Table S1	This study	BioSample: SAMD00224685 to SAMD00224700
Oligonucleotides		
Primer forward 342F: 5′-CTACGGGGGGCAGCAG-3′	Mori et al., 2014	https://doi.org/10.1093/dnares/dst052
Primer reverse 806R: 5′-GGACTACCGGGGTATCT-3′	Mori et al., 2014	https://doi.org/10.1093/dnares/dst052
Software and algorithms		
fastq-join v. 1.1.2–537	Aronesty, 2013	https://doi.org/10.2174/1875036201307010001
cutadapt v. 1.1	Martin, 2011	https://doi.org/10.14806/ej.17.1.200
Trimmomatic v. 0.32	Bolger et al., 2014	https://doi.org/10.1093/bioinformatics/btu170
EzBioCloud Microbiome Taxonomic Profiling pipeline	ChunLab; Kim et al., 2012; Yoon et al., 2017	https://www.ezbiocloud.net/contents/16smtp; https://doi.org/10.1099/ijs.0.038075-0 https://doi.org/10.1099/ijsem.0.001755
EzBioCloud 16S rRNA gene sequence database v. PKSSU4.0	ChunLab; Kim et al., 2012; Yoon et al., 2017	https://help.ezbiocloud.net/mtp-pipeline/; https://doi.org/10.1099/ijs.0.038075-0 https://doi.org/10.1099/ijsem.0.001755

(*Continued on next page*)

Continued

REAGENT or RESOURCE	SOURCE	IDENTIFIER
EzBioCloud curated chimera-free reference database	ChunLab	https://help.ezbiocloud.net/mtp-pipeline/
USEARCH v.8.1.1861_i86linux32	Edgar, 2010	https://doi.org/10.1093/bioinformatics/btq461
UCHIME in the USEARCH package as mentioned above	Edgar et al., 2011	https://doi.org/10.1093/bioinformatics/btr381
Chao1	Chao, 1984	https://www.jstor.org/stable/4615964
Non-parametric Shannon's index	Chao and Shen, 2003	https://doi.org/10.1023/A:1026096204727
Good's coverage of library	Good, 1953	https://doi.org/10.1093/biomet/40.3-4.237
generalized UniFrac distance	Chen et al., 2012	https://doi.org/10.1093/bioinformatics/bts342
Permutational Multivariate Analysis of Variance (PERMANOVA)	Anderson, 2017	https://doi.org/10.1002/9781118445112.stat07841
Other		
pH meter D-71	HORIBA	Cat# D-71S
Conductivity meter ES-51	HORIBA	Cat# ES-51
SOLAAR S Series AA spectrometer	Thermo Fisher Scientific	https://www.thermofisher.com/jp/en/home/industrial/spectroscopy-elemental-isotope-analysis.html
UV–160	Shimadzu	https://www.shimadzu.com/an/products/molecular-spectroscopy/index.html
761 Compact IC	Metrohm	https://www.metrohm.com/ja-jp/products-overview/17610010
TOC Analyzer TOC-VCPH	Shimadzu	https://www.shimadzu.eu/total-organic-carbon-analysis
Determination of Na^+, K^+, Ca^{2+}, Mg^{2+}, NH_4^+, Cl^-, NO_2^-, NO_3^-, SO_4^{2-}, and PO_4^{3-} concentrations	Japanese Industrial Standard (JIS) methods: JIS K 0102 48.2; JIS K 0102 49.2; JIS K 0102 50.2; JIS K 0102 51.2; JIS K 0102 42.2; JIS K 0102 35.3; JIS K 0102 43.1.2; JIS K 0102 43.2.5; JIS K 0102 41.3; JIS K 0102 46.1.3	https://webdesk.jsa.or.jp/books/W11M0090/index/?bunsyo_id=JIS+K+0102%3A2016
Determination of total nitrogen, total phosphorus, and total organic carbon	Japanese Industrial Standard (JIS) methods: JIS K 0102 45.2; JIS K 0102 46.3.1; JIS K 0102 22.1	https://webdesk.jsa.or.jp/books/W11M0090/index/?bunsyo_id=JIS+K+0102%3A2016
Beads Crusher μT-12	TAITEC	Cat# 0068700-000
Sterivex-GV 0.22 μm PVDF	Millipore	Cat# SVGV010RS
Luer lock	Millipore	Cat# XX3002564
Silicone pump tube	Yamamoto Scientific	Cat# 96400-25
Quantitative liquid feed pump	EYELA TOKYO RIKAKIKAI	Cat# RP-1000

RESOURCE AVAILABILITY

Lead contact

Further information and requests for reagents and resources should be directed to and will be fulfilled by the lead contact, Hironori Niki (hniki@nig.ac.jp).

Materials availability

This study did not generate unique reagents.

Data and code availability

The sequence datasets (n = 16) generated during this study are available at the DDBJ Sequence Read Archive (DRA) under accession number DRA010176. The associated BioProject and BioSample numbers are PRJDB8727 and SAMD00224685 to SAMD00224700, respectively.

EXPERIMENTAL MODEL AND SUBJECT DETAILS

Sample collection

Radial-type marimo samples of *Aegagropila linnaei* were collected on 5 August 2014 at Churui Bay in Lake Akan (43° 27′ N 144° 06′ E), Hokkaido, Japan. Small (about 4 cm in diameter, n = 3), medium (11 to 12 cm, n = 3), and large (21 and 22 cm, n = 2) samples were collected by scuba divers. Each sample was immediately transferred to a researcher in a boat. The samples were dissected on the boat; the outer surface and inner sections (~1.5 cm × ~1.5 cm × ~0.5 cm portions) used for DNA extraction were picked apart using sterilized tweezers and were separately placed in sterilized tubes; the samples for RNA extraction were also picked apart and immersed in RNA*later*® (Thermo Fisher Scientific, Waltham, MA). The outer sections of the small, medium, and large samples were labeled Radi-SO, Radi-MO, and Radi-LO, respectively; the inner sections were labeled Radi-SI, Radi-MI, and Radi-LI. All samples were transported to the lakeside laboratory and stored at –80°C until analysis. The samples in RNA*later*® were kept at 4°C overnight and then deep-frozen. To characterize microorganisms associated with radial-type marimo, floating *A. linnaei* filaments (labeled Fil) and tangled-type marimo of about 5 cm in diameter (n = 3) were collected for comparative analysis at Takiguchi Bay in Lake Akan. The tangled-type samples were dissected into the outer surface and inner sections in a similar manner as for the radial-type marimo, and were then labeled Tang-O and Tang-I, respectively. Additionally, surface lake water (labeled LW) and three samples of sediment (labeled Sed-1, Sed-2, and Sed-3) surrounding marimo colonies were collected. These samples were stored as described above. Further details of the sample codes are presented in Table S1.

METHOD DETAILS

Evaluation of lake water quality

The pH and electrical conductivity of the lake surface water were measured using a pH meter (D-71; Horiba, Kyoto, Japan) and a conductivity meter (ES-51; Horiba), respectively. The additional analyses described below were performed at Chikyu Kagaku Kenkyusho Co., Ltd. (Geo-Science Laboratory, Nagoya, Japan) following the Japanese Industrial Standard (JIS) methods (see Key Resources Table). The concentrations of Na^+, K^+, Ca^{2+}, and Mg^{2+} were determined using an atomic absorption spectrometer (SOLAAR S Series; Thermo Fisher Scientific). The concentration of NH_4^+ was measured by indophenol blue absorptiometry (UV–160; Shimadzu, Kyoto, Japan). The concentrations of Cl^-, NO_2^-, NO_3^-, SO_4^{2-}, and PO_4^{3-} were determined by ion chromatography (761 Compact IC; Metrohm, Herisau, Switzerland). To determine the total nitrogen concentration, the water sample was digested with potassium persulfate and was analyzed by UV-spectrophotometry (UV–160; Shimadzu). Total phosphorus was determined by standard molybdenum-blue colorimetry following persulfate digestion. Total organic carbon was measured using a TOC Analyzer (TOC-VCPH; Shimadzu).

DNA extraction, PCR amplification, and high-throughput sequencing

DNA was extracted from natural marimo samples using a modified version of the bead-beating method described previously (Nakai et al., 2012). A 0.5-g sub-sample was placed in a Lysing Matrix E Tube (MP Biomedicals, Santa Ana, CA), and then lysis solutions of an ISOIL for Beads Beating Kit (Nippon Gene, Toyama, Japan) were pre-warmed at 65°C and added to the tube according to the manufacturer's manual. After shaking in a Beads Crusher μT-12 (Taitec, Saitama, Japan) at 3200 rpm for 45 s, the tube was incubated at 65°C for 1 h, followed by centrifugal separation. DNA was purified from the aqueous supernatant using a MagExtractor™ Genome Kit (Toyobo, Osaka, Japan). The above procedure was conducted three times for each sample of each size, and the extracted DNAs were pooled by each size group (that is, small, medium, or large) to create a representative DNA sample. PCR amplicons were generated using the universal primer set 342F-806R (Mori et al., 2014), covering both archaeal and bacterial 16S rRNA genes. The PCR mixture containing KAPA HiFi HotStart ReadyMix (Kapa Biosystems, Wilmington, MA), reaction conditions, and sequencing library generation followed the 16S Metagenomic Sequencing Library Preparation

protocol provided by Illumina (San Diego, CA, USA). Pair-end 300-bp MiSeq (Illumina) sequencing was performed using a Nextera XT Index Kit (Illumina). DNA from comparative samples was extracted as outlined above. For the lake water, a 2000-ml sample was filtered onto a Sterivex Filter Unit with 0.22 μm pore size (Millipore, Billerica, MA) by using a Quantitative Liquid Feed Pump (RP-1000; EYELA, Tokyo) and a sterilized silicone tube (Yamato Scientific, Tokyo) with Luer-Lock fittings (Millipore). DNA extraction from the Sterivex unit was performed using a PowerWater Sterivex DNA Isolation Kit (MP Biomedicals). Each DNA sample was then PCR-amplified and sequenced as described above.

RNA extraction and cDNA synthesis

The internal multi-layers composed of sediment particles were observed only in the two large-sized, radial-type marimo samples. The three layers, the surface, intermediate and innermost layer, were used in order from the surface to the innermost layer for RNA extraction. The parts of each layer submersed in RNA*later*® were picked apart and labeled Radi-L1 (about 0.3 to 0.4 cm deep from the surface), Radi-L2 (1 cm deep), and Radi-L3 (2 cm deep), respectively. Total RNA was extracted from 0.5 g of each layer using a FastRNA® Pro Soil-Direct Kit (MP Biomedicals), as per the manufacturer's instruction. Residual DNA was digested using a TURBO DNA-*free*™ Kit (Thermo Fisher Scientific). The absence of DNA contamination was confirmed as the absence of PCR amplification of the digested template using the universal primer set 342F-806R as indicated above. The RNA was reverse-transcribed into cDNA using a SuperScript® VILO cDNA Synthesis Kit and Master Mix (Thermo Fisher Scientific), including random primers. The above procedure was performed three times for each sample, and the cDNAs from each layer group were pooled. Each cDNA was PCR-amplified and sequenced as described in the "DNA extraction" section.

Data analysis

The adapter sequences as well as ambiguous sequences that had a low average quality score (<25) were removed using cutadapt v. 1.1 (Martin, 2011) and Trimmomatic v. 0.32 (Bolger et al., 2014). The trimmed pair-end reads were assembled using fastq-join v. 1.1.2–537 (Aronesty, 2013). Taxonomic assignment of the quality-filtered sequences was processed with the default settings in the Microbiome Taxonomic Profiling (MTP) pipeline of the EzBioCloud (https://www.ezbiocloud.net/contents/16smtp; ChunLab Inc., Seoul, Korea) (Yoon et al., 2017). The quality-filtered sequences were compared to the EzBioCloud 16S rRNA gene sequence database v. PKSSU4.0 constructed from the curated 16S rRNA gene sequences using the USEARCH program v.8.1.1861_i86linux32 (Edgar, 2010). It is noted that, in this database, the yet-uncultured phylotype is tentatively given the hierarchical name assigned to the DDBJ/ENA/GenBank accession number with the following suffixes: "_s" (for species), "_g" (genus), "_f" (family), "_o" (order), "_c" (class) and "_p" (phylum) (Kim et al., 2012). The taxonomic category was assigned based on the following cut-off values of sequence similarity: species ($\geq$97%), genus (>97% > x $\geq$94.5%), family (>94.5% > x $\geq$86.5%), order (>86.5% > x $\geq$82%), class (>82% > x $\geq$78.5%), and phylum (>78.5% > x $\geq$75%), where x corresponds to the sequence identity with sequences in the database. These cut-off values were taken from previous studies (Yarza et al., 2014; Yoon et al., 2017). The sequences below the cut-off value at the species or a higher level were assigned in the unclassified group labeled as "_uc" (for unclassified). Chimeras of the sequences that did not match at the species level ($\geq$97%) were identified using the UCHIME program within USEARCH (Edgar et al., 2011) and the EzBioCloud chimera-free reference database (https://help.ezbiocloud.net/mtp-pipeline/), and chimeric sequences were omitted. Unmatched and eukaryotic plastid sequences were also excluded. The filtered valid sequences were used as the final dataset. Operational taxonomic units (OTUs) at a 97% identity threshold were picked up by the open-reference method (https://help.ezbiocloud.net/mtp-pipeline/) using the EzBioCloud MTP pipeline. Singleton sequences were removed in the OTU picking process, according to Unno (2015). Chao1 and non-parametric Shannon's indices and Good's coverage were used to estimate α-diversity indices (note that the chao1 index takes singleton reads into account), whereas β-diversity was expressed as generalized UniFrac distance (Chen et al., 2012). The α- and β-diversity indices were computed in the MTP pipeline.

QUANTIFICATION AND STATISTICAL ANALYSIS

Statistical analysis was performed in the EzBioCloud MTP pipeline as mentioned above. Permutational Multivariate Analysis of Variance (PERMANOVA) was used to compare the microbiome groups obtained from the generalized UniFrac dendrogram. A p value of <0.05 was considered significant.